Pathway complexity in supramolecular polymerization

Peter A. Korevaar, Subi J. George, Albert J. Markvoort, Maarten M. J. Smulders, Peter A. J. Hilbers, Albert P. J. J. Schenning, Tom F. A. De Greef, and E. W. Meijer

Nature **2012**, *481*, 492–496.

1. Introduction

1.1. Self-assembly processes under kinetic control

• Self-assembly has been used for preparation of functional materials; films, fibers, etc.

• Quantitative study has not been investigated sufficiently. Especially elucidation of mechanism by studying self-assembly process under kinetic control is necessary.

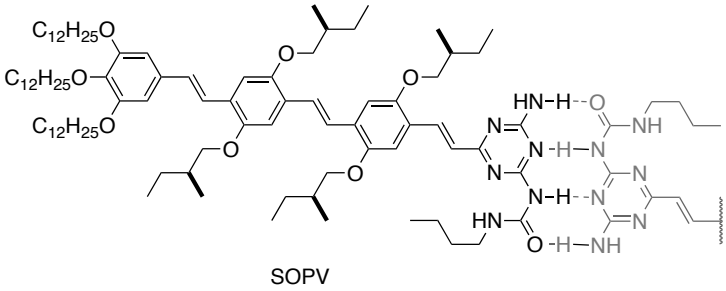

Figure 1. Molecular structure and hydrogen-bonded dimerization of SOPV.

1.2. Previous work

• *S*-chiral oligo(p-phenylenevinylene) (SOPV) serves as a functional material in a variety of organic electronic devices (ref. 1).

• Formation of one-dimensional right-handed helical structure, ***M*-SOPV** from hydrogen-bonded dimers of SOPV under thermodynamic control (Fig. 1, ref. 2) was demonstrated.

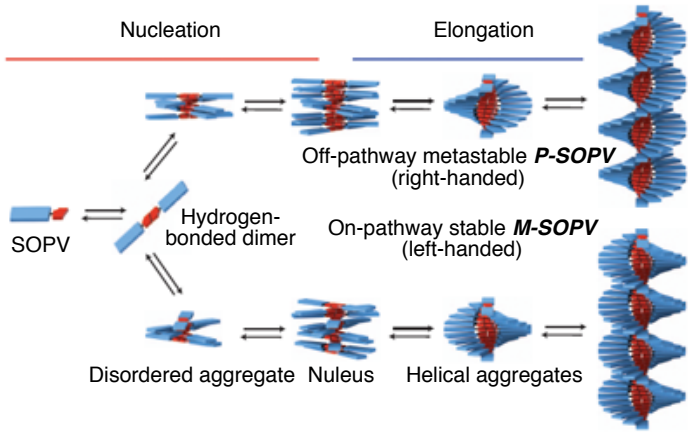

Figure 2. Schematic representation of the aggregation pathway of SOPV.

1.3. This work (Fig. 2)

• Self-assembly process of SOPV under kinetic control was studied.

• It was discovered that left-handed *P*-SOPV can form under kinetic control.

• The revealed self-assembly process includes two pathways; on-pathway and off-pathway, which generate *M*-SOPV and *P*-SOPV respectively.

• This work is composed of (i) observation of the self-assembly process under kinetic control, (ii) mechanistic analysis by modeling, and (iii) selective generation of the metastable structure, *P*-SOPV.

2. Results and Discussion

2.1. Preparation and characterization of SOPV aggregates formed under kinetic control

• A supramolecular structure under kinetic control was prepared by "stopped-flow experiments"(Scheme 1).

Scheme 1. Experimental procedures to obtain metastable aggregates

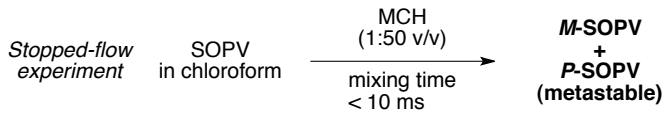

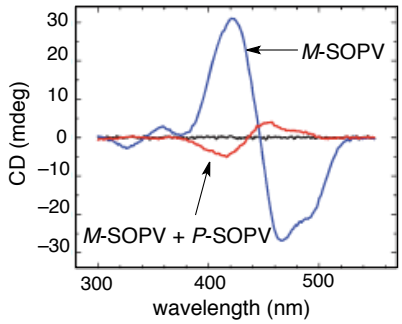

Figure 3. CD spectra of thermodynamically stale *M*-SOPV and mixture of *M*-SOPV and metastable *P*-SOPV.

• The quick mixing of SOPV solution in chloroform with a poor solvent, methylcyclohexane (MCH) afforded a mixture of *M*-SOPV and *P*-SOPV.

➜ Observation of *P*-SOPV by CD spectra (Fig. 3)

• To study the aggregation kinetics after the mixing, time-resolved CD spectra were measured.

• Influence of concentration and temperature on time change of CD spectra was studied (Fig. 4).

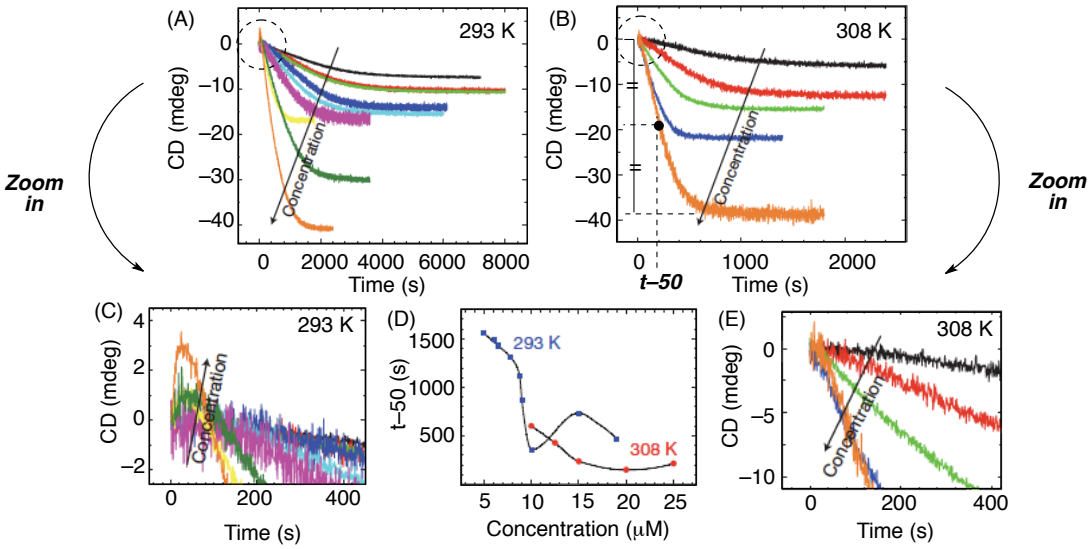

Figure 4. Concentration-dependent kinetics analyzed by CD spectra (λ = 466 nm) (A) at 293 K (B) at 308 K(C) Zoom in for panel A. (D) *t*–50 vs. concentration at 293 K and 308K. (E) Zoom in for panel B.

• Fig. 4A indicate increase of thermodynamically stable *M*-SOPV as the time advances. However, the situation was different at the initial stage (Fig. 4C).

– A positive CD signal at higher concentrations suggests formation of *P*-SOPV.
– The tendency was also observed under the heated condition (Fig. 4B,E).)

• For further analysis, time parameter "*t*–50" at which 50% of the aggregation process completes (illustrated in Fig. 4B) was determined. Small *t*–50 means fast formation of thermodynamically stable *M*-SOPV.

• A unique tendency was observed:

– At 293 K, M-SOPV formed faster (that is, smaller *t*–50) at 10 μM than at 15 μM (Fig. 4D).
– The shortest *t*–50 time shifts to a higher SOPVconcentration (10 μM at 293 K ➜ 20 μM at 306 K).

➜ Mechanistic study was carried out by simulation.

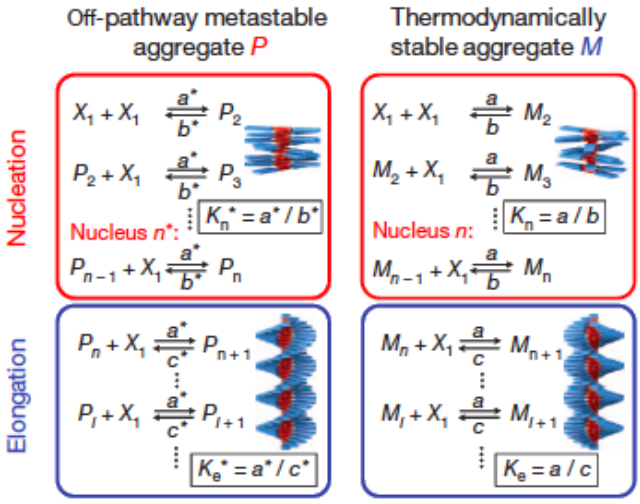

Figure 5. Schematic representation of reversible kinetic model for nucleated supramolecular polymerization. X_1: Hydrogen-bonded dimer, P_n, M_n: *P*-/*M*-type aggregates with aggregation number of n.

2.2. Rationalization of the experimental aggregation kinetics

• The mechanism was studied based on protein fibrillation models (Fig. 5, ref. 3).

• The model considers two aggregation pathways; **on-pathway** leading to thermodynamically stable aggregates and **off-pathway** leading to kinetically stable aggregates.

• The model only assumes monomer association and dissociation for size change of aggregates. Therefore the transition from metastable to thermodynamically stable aggregates was assumed to occur via depolymeriation of *P*-SOPV and subsequent growth of *M*-SOPV.

[Results of the simulation]

• Simulation with the model showed that the *P*-SOPV aggregates only appear in the initial stages of the self-assembly process if sufficient monomers are present.

– When $a^* > a$, the kinetic model successfully described the experimental data (Fig. 6A).
– Calculated Gibbs free energy (Fig. 6B) revealed that the *P*-SOPV nucleus is thermodynamically more stable than the *M*-SOPV nucleus (that is, $K_n^* > K_n$), while *M*-SOPV is more stable in the elongation phase.

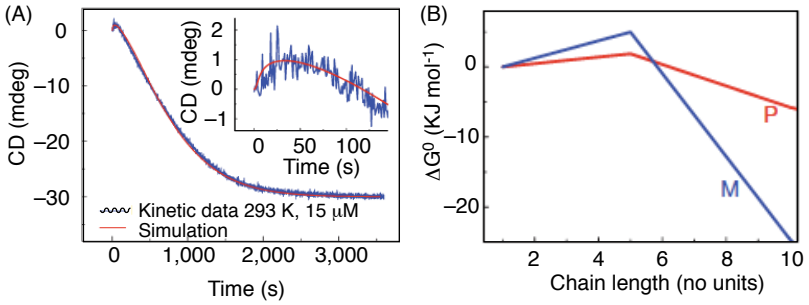

Figure 6. Results of calculation based on the kinetic model. (A) Change of CD spectra matches with the experimental data when $a^* > a$. (B) Calculated Gibbs free energy diagram indicating $K_n^* > K_n$.

• The changes in the $t - 50$ values with concentration could be rationalized by taking off-pathway into account (Fig. 7A, B).

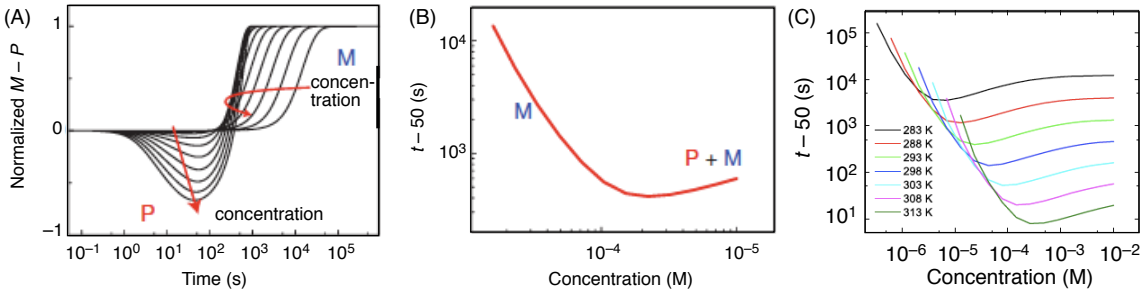

Figure 7. Description of the aggregation process by taking off-pathway aggregation in account. (A) Concentration-dependent simulation of kinetics with pathway competition model. (B) *t*-50 vs. SOPV dimer concentration obtained from simulation.(C) Temperature-dependent sumu-lations with pathway copetition model.

– At higher concentrations, larger amount of *P*-type nuclei are formed.
– *P*-type nuclei consume monomers, inhibiting the formation of the thermodynamically stable *M*-type aggregates.
– Simulations exploring the effect of temperature showed that the aggregation rate gets faster upon increasing the temperature (thus, lower $t - 50$) (Fig. 7C).

➜ Correspondence to the experimental results (cf. Fig. 4D)

2.3. Direction of assembly of SOPV toward metastable products

• Based on the mechanism, they attempted to force the assembly of SOPV into exclusively *P*-type aggregates.

• Previous studies have shown that carboxylic acid groups can bind to OPV dimers via hydrogen bonding (ref. 4).

• When DTA, a chiral dicarboxylic acid was added to SOPV, a *P*-type helical aggregate (*P*-DTA-SOPV) generated selectively (Scheme 2).

Scheme 2. Stabilizaition of *P*-type helical aggregate by addition of DTA

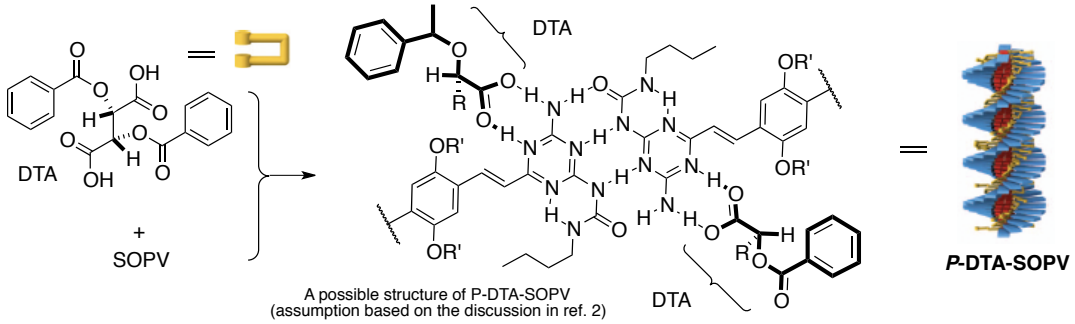

A possible structure of P-DTA-SOPV
(assumption based on the discussion in ref. 2)

• The opposite helicity of *P*-DTA-SOPV compared to equilibrium conditions (*M*-SOPV) was demonstrated by the opposite CD spectrum (Fig. 8).

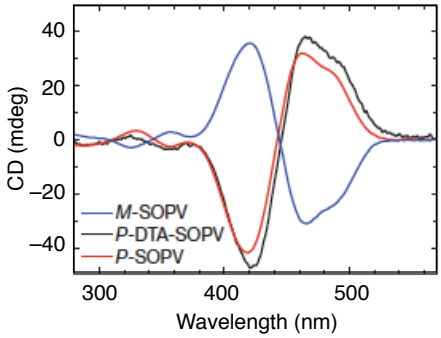

Figure 8. CD spectra of *M*-SOPV, *P*-DTA-SOPV, and *P*-SOPV.

• Pure *P*-SOPV was obtained by "two-step non-covalent synthetic methodology"(Fig. 9A)
– STEP 1) Formation of *P*-DTA-SOPV
– STEP 2) Removal of DTA from the SOPV aggregates by aqueous extraction at 273 K using ethyl diamine

➜ Transiently stable *P*-SOPV was formed.

• In addition, the kinetic lability of *P*-SOPV is demonstrated by annealing at 298 K, resulting in a time-dependent stereomutation of the CD spectra indicative of a conversion from *P*-SOPV towards *M*-SOPV aggregates (Fig. 9B).

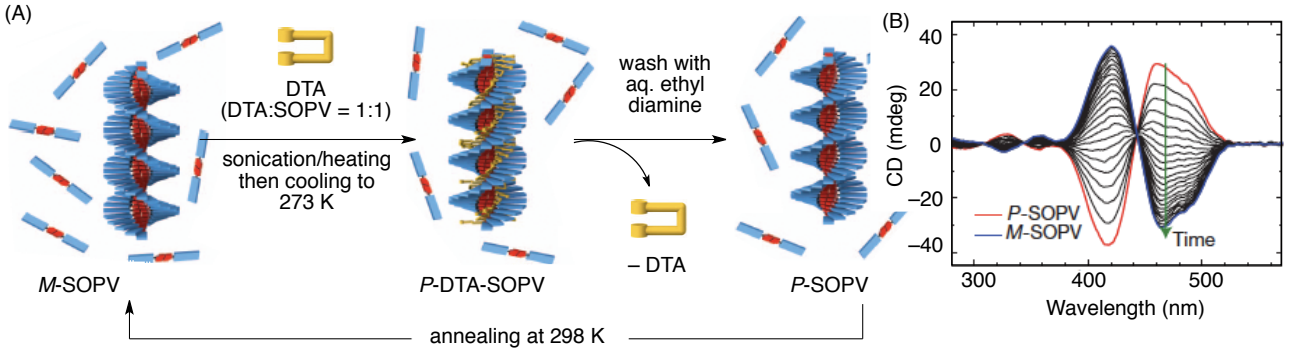

Figure 9. Preparation of pure *P*-SOPV via a two-step non-covalent synthetic methodology. (A) Schematic repre-sentation of the procedure. (B) Change of CD spectra upon conversion from *P*-SOPV to *M*-SOPV upon annealing.

3. Conclusion

• The aggregation of SOPV involves two competing pathways leading to assemblies with opposite helicity, one of which is favored kinetically (*P*-SOPV) and the other thermodynamically (*M*-SOPV).

• This work reveals that the influence of the metastable state on the overall assembly process is mediated through the equilibrium with free monomers.

• The effect is a common mechanism for one-dimensional supramolecular systems, and would be applicable to almost all organic materials.

• By influencing the self-assembly process through tuning of the on-pathway or off-pathway mechanisms, the resulting morphologies could potentially be controlled to arrive at optimized self-assembled functional materials.

4. References

1. Hoeben, F. J.; M. Jonkheijm, P.; Meijer, E. W.; Schenning, A. P. H. J.; *Chem. Rev*. **2005**, *105*, 1491–1546.
2. Jonkheijm, P.; van der Schoot, P.; Schenning, A. P. H. J.; Meijer, E. W. *Science* **2006**, *313*, 80–83.
3. Poers, E. T.; Powers, D. L. *Biophys. J*. **2008**, *94*, 379–391.
4. George, S. J.; Tomovi´c, Z.; Smulders, M. M. J.; de Greef, T. F. A.; Leclè, P. E. L. G, Meijer, E. W.; Schenning, A. P. H. J. *Angew. Chem. Int. Ed.* **2007**, *46*, 8206–8211.